Ecological Complexity 60 (2024) 101104

Contents lists available at ScienceDirect

Ecological Complexity

journal homepage: www.elsevier.com/locate/ecocom

A scale-invariant method for quantifying the regularity of environmental spatial patterns

Karl Kästner [a,*], Roeland C. van de Vijsel [b], Daniel Caviedes-Voullième [c,d], Christoph Hinz [a]

[a] Hydrology, BTU Cottbus-Senftenberg, 03046 Cottbus, Germany
[b] Hydrology and Environmental Hydraulics Group, Wageningen University, 6708 PB Wageningen, The Netherlands
[c] Institute of Bio- and Geosciences: Agrosphere (IGB-3), Forschunszentrum Jülich, 52428 Jülich, Germany
[d] Simulation and Data Lab Terrestrial Systems, Jülich Supercomputing Centre (JSC), 52425 Jülich, Germany

ARTICLE INFO

Dataset link: https://github.com/karlkastner/environmental-spatial-patterns-metastudy, https://zenodo.org/records/13974157

Keywords:
Self-organization
Scale-dependent feedback
Arid vegetation
Stochastic processes
Turing pattern
Spectral analysis

ABSTRACT

Spatial patterns of alternating high and low biomass occur in a wide range of ecosystems. Patterns can improve ecosystem productivity and resilience, but the particular effects of patterning depend on their spatial structure. The spatial structure is conventionally classified as either regular, when the patches of biomass are of similar size and are spaced in similar intervals, or irregular. The formation of regular patterns is driven by scale-dependent feedbacks. Models incorporating those feedbacks generate highly regular patterns, while natural patterns appear less regular. This calls for a more nuanced quantification beyond a binary classification. Here, we propose measuring the degree of regularity by the maximum of a pattern's spectral density, based on the observation that the density of highly regular patterns consists of a narrow and high peak, while the density of highly irregular patterns consists of a low and wide lobe. We rescale the density to make the measure invariant with respect to the characteristic length-scale of a pattern, facilitating the comparison of patterns observed or modelled under different conditions. We demonstrate our method in a metastudy determining the regularity of natural and model-generated patterns depicted in previous studies. We find that natural patterns have an intermediate degree of regularity, resembling random surfaces generated by stochastic processes. We find that conventional deterministic models do not reproduce the intermediate regularity of natural patterns, as they generate patterns which are much more regular and similar to periodic surfaces. We call for appreciating the stochasticity of natural patterns in systems with scale-dependent feedbacks.

1. Introduction

A wide range of ecosystems exhibit spatial patterns where the biomass is concentrated in patches (Rietkerk and van de Koppel, 2008). Such patterns have received considerable attention, as they can improve ecosystem productivity and resilience under increasing environmental pressure (Rietkerk et al., 2021). Two classes of patterns are distinguished, regular patterns, where the size of patches and the distance between patches has a characteristic length scale, and irregular patterns, where this is not the case (Klausmeier, 1999; von Hardenberg et al., 2010; Kéfi et al., 2010). Regular patterns in particular, yield fascinating images when captured from air and space (Fig. 1a,b). They include a.o. patterns of vegetation in drylands (Lejeune et al., 2004), fairy rings in savannahs (Bonachela et al., 2015), patterns in mussel beds (van de Koppel et al., 2005), in freshwater marshes (van de Koppel and Crain, 2006), in seagrass meadows (van der Heide et al., 2010), in stream vegetation (Cornacchia et al., 2018), and algae biofilms in intertidal areas (Weerman et al., 2010; van de Vijsel et al., 2020).

Ecosystems facilitate human life but are under increasing pressure by local and global changes, including those of land use and climate. Spatial patterning has been suggested as an indicator of ecosystem health, in particular as a sign of imminent critical transitions, such as sudden desertification (Kéfi et al., 2007; Scheffer et al., 2009; Weerman et al., 2012; Kefi et al., 2014; Bonachela et al., 2015). However, patterning can also increase the ecosystem productivity and resilience against environmental pressure (Rietkerk et al., 2021). The relation between patterns and ecosystem health is complex: alternative stable states can exist under the same environmental conditions (Bastiaansen et al., 2018), or even coexist in different parts of a pattern (Zelnik and Meron, 2018), responses to environmental change can be gradual or sudden (Bel et al., 2012). Sustainable ecosystem management thus requires a thorough understanding of a pattern's structure and pattern-forming processes.

* Corresponding author.
E-mail address: kastner.karl@gmail.com (K. Kästner).

https://doi.org/10.1016/j.ecocom.2024.101104
Received 21 August 2023; Received in revised form 31 July 2024; Accepted 3 September 2024
Available online 30 October 2024

The formation of regular patterns in resource limited ecosystems has been attributed to self-organization driven by short range facilitation and long range competition between the pattern-forming organisms (Rietkerk and van de Koppel, 2008; Borgogno et al., 2009; Meron, 2015). Regular patterns can be generated with mathematical models (Fig. 1c,d) which either phenomenologically account for the interaction (Thiery et al., 1995; Dunkerley, 1997; Lefever and Lejeune, 1997; Lejeune et al., 1999), or explicitly mimic bio-physical processes (Klausmeier, 1999; Hille Ris Lambers et al., 2001; Rietkerk et al., 2002; van de Koppel et al., 2005; van de Koppel and Crain, 2006; Gilad et al., 2007; Siteur et al., 2014b; Bonachela et al., 2015). Regular environmental spatial patterns are conceptually understood to be periodic, which has been corroborated by mathematical models which generate highly regular patterns (Meron, 2015; Fernandez-Oto et al., 2019; Caviedes-Voullième and Hinz, 2020; Bera et al., 2021; Clerc et al., 2021; Inderjit et al., 2021; Rietkerk et al., 2021; Kabir and Gani, 2022; Siteur et al., 2023; Bennett et al., 2023). The terms regular and periodic are rarely differentiated in the literature on spatial patterns. For clarity, we distinguish periodic and regular patterns based on the definition of Kästner et al. (2024): A periodic pattern is identical to itself when shifted in space in intervals corresponding to its characteristic wavelength λ_c along one of its axes of symmetry, and therefore can be cut into identical tiles. A periodic pattern is consequently globally correlated, i.e. its autocorrelation function oscillates with constant amplitude at the characteristic wavelength. Conversely, the spectral density of a periodic pattern consists of narrow and high peaks at their characteristic wavenumber. For patterns with a finite spatial extent, the height of the peaks is proportional to the area of the pattern. The periodic spatial structure is retained and evident in the spectrum and autocorrelation, even when it is randomly perturbed, e.g. by adding noise or by locally varying the patches. A regular pattern appears similar, but not identical, to itself when shifted in space in intervals corresponding to its characteristic wavelength. When cut into tiles with side lengths corresponding to the characteristic wavelength, neighbouring tiles are similar, but the similarity between two tiles decreases the further they are separated. The pattern consequently decorrelates with increasing distance, i.e. the autocorrelation function has maxima at multiples of the characteristic wavelength, but the height of the maxima decreases with increasing lag distance. Conversely, the spectral density is lobed, reaching its maximum at its characteristic wavenumber. The height and the width of the lobe depend on the regularity of the pattern, but not on its spatial extent. A periodic pattern can be perturbed locally by varying patches or superimposing noise, i.e. by adding non-periodic components. However, the spatial structure of the periodic components remains distinct in the autocorrelation function and the spectral density.

Natural regular patterns exhibit a considerable degree of random variation: the distance between patches as well as the size of patches vary, and the fringes of patches are frayed (Fig. 1a,b). This variation is not reproduced in patterns generated by conventional mathematical methods (Fig. 1c,d). Recently, Kästner et al. (2024) revisited classifications of environmental spatial patterns. Using a large global dataset, they showed that natural regular patterns are in general not periodic, and suggested they have an intermediate degree of regularity. This finding reveals the need for a method to quantify the degree of regularity beyond the binary classification as periodic or not and for a thorough investigation of the differences between model-generated and natural patterns.

There are various methods for analysing point patterns consisting of isolated individuals such as trees, or continuous patterns consisting of patchy vegetation such as shrubs, c.f. Dale (2000). Regular patterns typically consist of patches and have historically been analysed with the blocked quadrat variance (Dale, 2000), or with spectral methods (Renshaw and Ford, 1984). However, so far, only the wavelength, but not the regularity of environmental spatial patterns has been studied systematically (Couteron, 2002; Deblauwe et al., 2011), likely, because regularity has so far been viewed as a binary property of either being periodic or not. Here, we recognize the regularity as a continuous property, which determines where a pattern is in between the extreme cases of a periodic surface (highest regularity) and patterns without finite characteristic length scale (lowest regularity). The regularity measures how similar a pattern is to itself when being shifted in space by a distance corresponding to its characteristic wavelength, i.e. how similar directly adjacent tiles are on average. The higher the regularity (Fig. 2a) the slower the oscillation of the autocorrelation decays, i.e. the more similar adjacent tiles appear. Periodic and irregular patterns are thus limit cases of regular patterns, where in the former case, the oscillation of the autocorrelation does not decay, and in the latter case the autocorrelation does not oscillate at all.

Several pattern properties related to regularity have been used as indicators of resilience with respect to environmental pressure. These include the size distribution of the patches (Kéfi et al., 2011) and distribution of the patch spacing (Bastiaansen et al., 2020), or defects in striped patterns, such as termination or branching of stripes (Pinto-Ramos et al., 2023). However, the patch size, interpatch distance and defects are unsuitable for measuring the correlation length and hence the regularity, since they are local properties Kästner et al. (2024).

Here, we propose measuring the regularity generically by the maximum of the mode spectral density (Fig. 2b), as it has advantageous statistical properties compared to the autocorrelation and patch-based statistics. The spectral density is uniquely related to the autocorrelation via the Fourier transform. We rescale the spatial dimensions to make the regularity estimate scale-independent, thus facilitating the pooling of the regularity of patterns within one group and comparing it against the regularity of patterns within another group. Our approach is similar to the method based on the width of the mode of the radial spectral density for measuring the degree of imperfection of labyrinthine patterns recently proposed by Echeverría-Alar et al. (2023). We then apply our method in a metastudy of over 60 publications on regular environmental spatial patterns, where we compare the regularity of the depicted natural and model-generated patterns.

This paper is structured as follows: First, we introduce a method for measuring the regularity for spatial patterns (Section 2.4). Second, we present the meta-analysis of environmental spatial patterns (Section 3). Lastly, we discuss implications for modelling environmental spatial patterns 4.

2. Methods

We estimate the degree of regularity from the spectral density of a pattern. The height of the mode, i.e. the maximum, of the density, when appropriately scaled, is a quantitative estimate of the degree of regularity, while the location of the mode is an estimate of the characteristic wavenumber. The spectral density has to be estimated from the periodogram, as it is not known in the general case. The periodogram consists of the squared magnitude of a pattern's frequency components. The frequency components of environmental spatial patterns (Fig. 1e-f) are randomly scattered, which indicates that the patterns are random surfaces generated by stochastic processes (Kästner et al., 2024). The scatter hinders a direct quantification of the regularity from the periodogram. To determine the regularity, the spectral density, which is the expected magnitude of the frequency components, has to be first estimated by smoothing, i.e. averaging neighbouring periodogram values or by fitting an appropriate parametric density model. However, even without smoothing, the regularity of a pattern can be visually assessed from the periodogram. This is because the spectral energy of highly regular patterns is concentrated in a narrow frequency range (Fig. 1g-h), while the spectral energy of less regular patterns is distributed over a larger frequency range (Fig. 1e-f). The estimated density is uncertain, and a trade-off between bias and variance has to be made. For environmental spatial patterns, we decompose the density in two-dimensional components, as this reduces the bias and facilitates

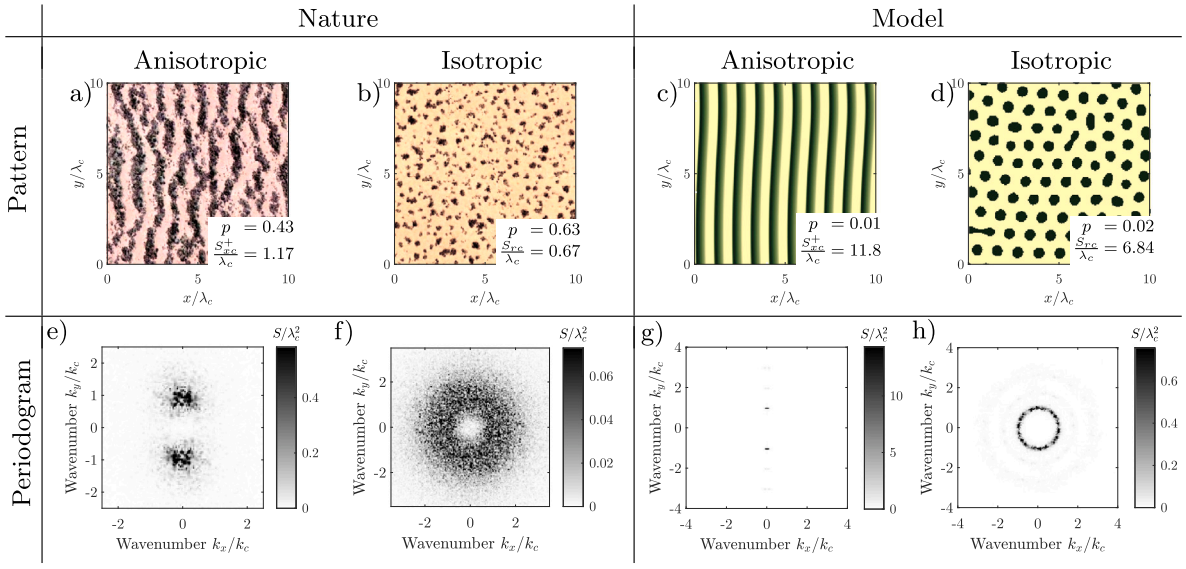

Fig. 1. Comparison of typical natural and model generated patterns. Both model generated and natural patterns have a regular spatial structure with a characteristic wavelength. However, model generated patterns are much more regular, as their spectral energy is concentrated in the characteristic frequency component, while the spectral energy of natural patterns is distributed over a wider range of frequencies. (a) A striped and (b) a spotted vegetation pattern captured in the Kordofan, Sudan (11°19'49"N 28°21'19"E, 2021 and 11°32'00"N, 27°55'40"E, 2021, Aerial images from Google Maps Maxar Technologies, CNES/Airbus). Their characteristic wavelengths are λ_c of 96 m and 102 m, respectively. The striped pattern has been rotated to align with the coordinate axes. $S_{xc}+/\lambda_c$ and S_{rc}/λ_c are the regularity of anisotropic and isotropic patterns, as defined in Section 2.4. p is p-value of the periodicity test (Kästner et al., 2024). (c) A striped and (d) a spotted pattern generated with the Rietkerk model (Rietkerk et al., 2002). Parameters for the spotted pattern: rainfall intensity R = 0.75 mm/d, surface water diffusivity e_h=100 m^2/d. Parameters for the striped pattern: R=1 mm/d, e_h=25 m^2/d, runoff velocity v_{hy} = 10 m/d. All simulations in this study were run in a square domain with a side length L = 1000 m and for a duration of 4 ·10^5 days ≈ 1100 years. (e–h) Corresponding rotated periodograms, showing how much of the spatial variance if contributed by each frequency component, c.f. Section 2. The spurious low-frequency components with wavenumbers $k \ll k_c$ have been suppressed in the periodograms of natural patterns. The coordinate axes, representing the wavenumber k_x in the direction perpendicular and k_y in the direction parallel to the stripes, are scaled by the characteristic wavenumber k_c, the wavenumber at which the spectral density reaches a maximum.

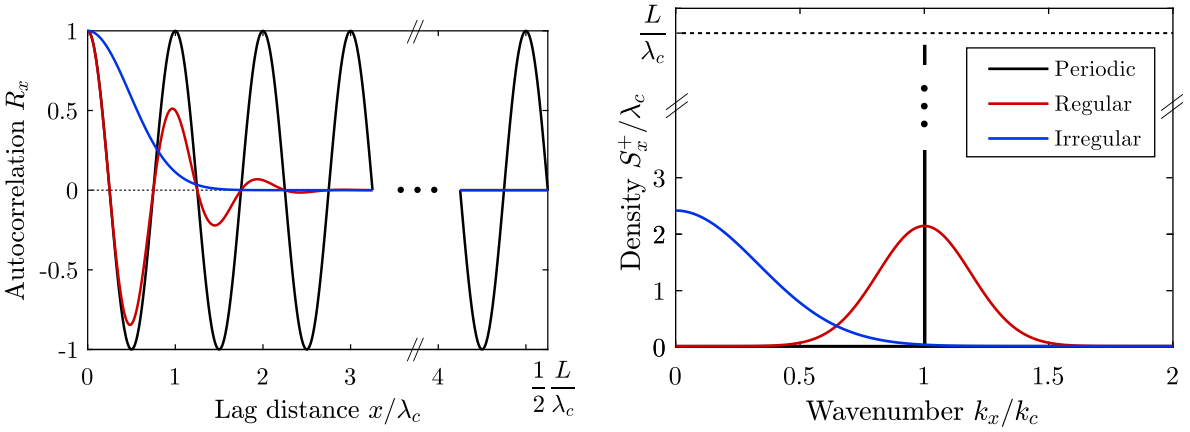

Fig. 2. Schematic comparison of the autocorrelation R and spectral density S of a periodic pattern, a regular stochastic pattern and an irregular pattern. (a) The autocorrelation of periodic patterns and stochastic regular patterns both oscillate at the characteristic wavelength λ_c. The oscillation of periodic patterns remains constant, as they remain correlated over their entire spatial extent, while the oscillation of stochastic patterns decays as the patterns decorrelate with increasing lag distance. The autocorrelation of irregular patterns decays without oscillating. (b) The spectral densities of both periodic and regular stochastic patterns have a maximum at the characteristic wavenumber k_c. For a periodic pattern, the value of the maximum is proportional to the spatial extent L of the pattern, while the maximum of a regular stochastic pattern is independent of the spatial extent. The maximum of irregular patterns occurs at the zero wavenumber.

the visual interpretation. Beside estimating the decomposed density, the estimation of the regularity requires two more steps: First, we normalize the periodogram similar to a probability density so that the estimate is independent of the spatial and spectral resolution, i.e. the pixel size and the spatial extent of the pattern. Second, we rescale the periodogram so that the regularity estimate is invariant with respect to the characteristic length scale of the pattern. Below, we first explain the method for the ideal case of a pattern with infinite spatial and spectral resolution, and then further explain the method for practical cases of patterns captured in satellite images with finite spatial resolution and finite spatial extent.

2.1. Decomposition of the two-dimensional spectral density

We start our analysis with the two-dimensional spectral density S_{xy} of a patterns biomass concentration b per unit area. The spectral density determines which fraction of the spatial variance σ_b each frequency component contributes:

$$S_{xy}(\vec{k}) = \frac{1}{\sigma_b^2}\left|\mathrm{E}\left[\left(b(\vec{x})-\bar{b}\right)\exp\left(-\mathrm{i}\,\vec{k}^T\,\vec{x}\right)\right]\right|^2, \tag{1a}$$

$$\sigma_b = E[(b(\vec{x})-\bar{b})^2], \tag{1b}$$

$$\bar{b} = E[b(\vec{x})]. \tag{1c}$$

Here, $\vec{x} = [x, y]^T$ is the spatial coordinate and $\vec{k} = [k_x, k_y]^T$ is the wavenumber. In general, the spatial structure is independent of the mean biomass $\bar{b}$.

We decompose the two-dimensional density into its axial components. When analysing anisotropic, i.e. striped, patterns, we first rotate the coordinate system so that the stripes of the pattern are on average perpendicular to the primary axis x. Then, we decompose the density into a component S_x perpendicular to the stripes (transect direction) and a component S_y parallel to the stripes by integrating in the respectively orthogonal direction (Fig. 3a):

$$S_x(k_x) = \frac{1}{2\pi} \int_{-\infty}^{\infty} S_{xy}(k_x, k_y)\, \mathrm{d}k_y, \tag{2a}$$

$$S_y(k_y) = \frac{1}{2\pi} \int_{-\infty}^{\infty} S_{xy}(k_x, k_y)\, \mathrm{d}k_x. \tag{2b}$$

The area of the one-dimensional densities S_x and S_y both integrates to 1, as the two-dimensional density S_{xy} has unit volume and is positive, i.e. $S_{xy} \geq 0$,

The density S_x is symmetric i.e. $S_x(k_x) = S_x(-k_x)$, as the two-dimensional density $S_{xy}(k_x, k_y) = S_{xy}(-k_x, -k_y)$ is symmetric. For regular patterns, S_x is bimodal, i.e. consists of two lobes with maxima at the characteristic wavenumber $\pm k_c > 0$. For sufficiently regular patterns, the modes are well separated from zero, i.e. $S_x(k_c) \gg S_x(0)$. We therefore introduce the density S_x^+, which only consists of the part along the positive half-axis. It is unimodal and can therefore be readily compared to the radial density and common unimodal densities without rescaling:

$$S_x^+(k_x) = \begin{cases} 2\, S_x(k_x), & k_x \geq 0, \\ 0, & k_x < 0. \end{cases} \tag{3a}$$

where the factor 2 ensures that S_x^+ has unit area as required for a density. While S_y is symmetric as well, we do not split it in half, as its mode is centred at zero.

When analysing isotropic patterns, i.e. spotted, labyrinthine and gapped patterns, we first transform the density into polar coordinates:

$$S_{r\theta}(k_r, \theta) = S_{xy}(k_r \cos(\theta), k_r \sin(\theta)), \tag{4}$$

where $k_r = \sqrt{k_x^2 + k_y^2}$ is the radial wavenumber and $\theta = \mathrm{atan}_2(k_x, k_y)$ the angle. The transformation retains the volume of the density at unity $(2\pi)^{-2} \int_0^{\infty} \int_{-\pi}^{\pi} k_r\, S_{r,\theta}\, \mathrm{d}\theta\, \mathrm{d}k_r = 1$ Then, we decompose the density into a radial component S_r and an angular component S_θ, by integrating along rings and infinitesimal sectors, respectively (Fig. 3b):

$$S_r(k_r) = \frac{1}{I_{r\theta}} \int_{-\pi}^{\pi} S_{r\theta}(k_r, \theta)\, \mathrm{d}\theta, \tag{5a}$$

$$S_\theta(\theta) = \frac{1}{2\pi^2} \int_0^{\infty} k_r\, S_{r\theta}(k_r, \theta)\, \mathrm{d}k_r, \tag{5b}$$

The angular density retains its unit area by the integration, i.e. $(2\pi)^{-2} \int_0^{\infty} k_r\, S_r\, \mathrm{d}k_r = 1$. The radial density has to be explicitly normalized with the factor $I_{r\theta} = (2\pi)^{-1} \int_0^{\infty} \int_{-\pi}^{\pi} S_{r\theta}(k_r, \theta)\, \mathrm{d}\theta\, \mathrm{d}k_r$. For fairly regular patterns, $I_{r\theta} \approx \lambda_c$.

The symmetry of the two-dimensional density carries over into polar coordinates, i.e. $S_{r\theta}(k_r, \theta) = S_{r\theta}(k_r, \theta + \pi)$. The angular density of anisotropic patterns is therefore bimodal with peaks at 0 and π. We therefore split the angular density S_θ in two symmetric components S_θ^+ and $S_\theta^-(\theta) = S_\theta^+(\theta + \pi)$ spanning each a half-circle and which can be readily compared to S_y and common unimodal densities without rescaling:

$$S_\theta^+(k_x) = \begin{cases} 2\, S_\theta(\theta), & -\pi/2 \leq \theta < \theta, \\ 0, & \text{otherwise.} \end{cases} \tag{6a}$$

Where the factor 2 again ensures that the area of the density is unity.

2.2. Reconstruction of the two-dimensional density

The two-dimensional density can be reconstructed from the product of the one-dimensional components up to a residual Res. For anisotropic patterns,

$$S_{xy}(k_x, k_y) = S_x(k_x)\, S_y(k_y) + Res_{xy}(k_x, k_y). \tag{7a}$$

The residual Res_{xy} is small, when the mode of the spectral density has elliptic contours and continuous derivatives at its maximum, and zero, when S_x and S_y are Gaussian. For isotropic patterns:

$$S_{r\theta}(k_r, \theta) = I_{r\theta}\, S_r(k_r)\, S_\theta(\theta) + Res_{r\theta}(k_r, \theta). \tag{7b}$$

The residual $Res_{r\theta}$ is small, when the angular density S_θ is flat. The residuals Res_{xy} and $Res_{r\theta}$ are not densities, because they integrate to zero, instead of unity, and because they are not strictly positive, but have equal positive and negative components. Any pattern can be decomposed and reconstructed either way, irrespectively if it is isotropic or anisotropic, or regular at all.

2.3. Rescaling of the spectral density

The density along the primary axis, i.e. S_x for anisotropic and S_r for isotropic patterns, has the local maximum S_{xc} or S_{rc}. The location of this maximum indicates the characteristic wavenumber k_c and with it the characteristic wavelength $\lambda_c = 2\pi/k_c$ of the pattern. We rescale the coordinates in real space by dividing the distance by the characteristic wavelength (Fig. 4). This yields the non-dimensional distance x/λ_c, wavenumber k/k_c and non-dimensional density $S_x \cdot k_c/(2\pi) = S_x/\lambda_c$, $S_{xy} \cdot k_c/(2\pi) = S_{xy}/\lambda_c^2$. The maximum of the rescaled density S_{xc}/λ_c or respectively S_{rc}/λ_c is independent of the wavelength and primarily an indicator of a pattern's regularity. The rescaling is only applicable to patterns when the characteristic wavenumber k_c is distinct from zero, and thus not for irregular patterns, so called scale-free patterns, where the maximum of the spectral density occurs at $k_c = 0$ or where the spectral density has no local maximum.

2.4. Definition of regularity

A pattern appears the more regular, the more of its spatial variance is contributed by frequency components with periods close to its characteristic wavelength λ_c. As the spatial variance is proportional to the spectral energy this lends itself to the following definition of the regularity of a one-dimensional pattern:

$$\mathrm{Regularity}_x = \frac{S_{xc}^+}{\lambda_c}. \tag{8}$$

We derive the definition in detail in the supplement, section 1.9. Rescaling with $1/\lambda_c$ ensures that the regularity S_{xc}^+/λ_c is scale-invariant. The regularity varies between the limit cases of a periodic pattern and irregular patterns. The regularity is infinite for periodic patterns with infinite spatial extent. The regularity is zero, for irregular patterns where the mode of the spectral density is centred at the origin or the density is flat. Among natural regular patterns, the regularity varies but is typically not far from 1.

We define the regularity of two-dimensional patterns as:

$$\mathrm{Regularity}_{xy} = 2\frac{S_{xyc}}{\lambda_c^2}. \tag{9a}$$

Anisotropic patterns appear the more regular, the larger the larger this value, c.f. Fig. 5d. S_{xyc} is the maximum value of the two-dimensional density S_{xy}. For anisotropic patterns, this is approximately equal to the product of the regularity of its two components, c.f. Eq. (7a):

$$\mathrm{Regularity}_{xy} \approx 2\frac{S_{xc} \cdot S_{yc}}{\lambda_c^2} = \frac{S_{xc}^+ \cdot S_{yc}}{\lambda_c^2}. \tag{9b}$$

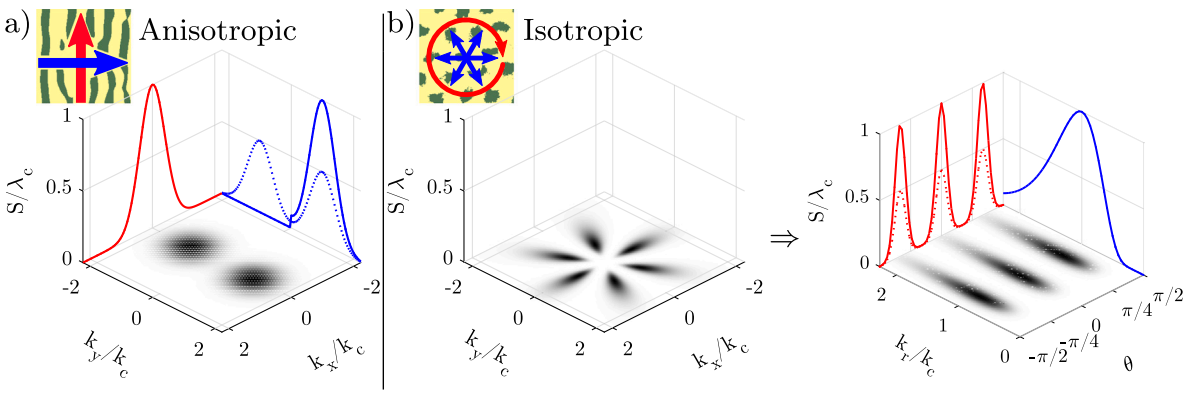

Fig. 3. Decomposition of the two-dimensional spectral density into two one-dimensional components. (a) Anisotropic pattern, solid line indicates the density along the positive half-axis S_x^+, dashed line the density over the full axis S_x (b) Isotropic pattern, solid line indicates the density over the half-circle S_θ^+, dashed line the density over the full circle S_θ. As the spectra are symmetric, we display only the part spanning the positive half-axis and half-circle further on.

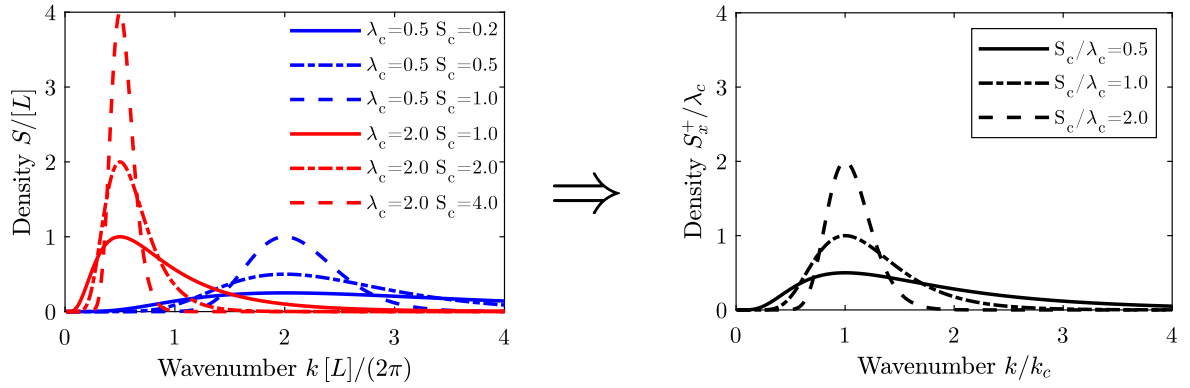

Fig. 4. Rescaling of a pattern results in a regularity measure that is independent of a pattern's scale. (a) Blue densities belong to patterns with the same characteristic wavelength 0.5 [L], but different regularity. [L] is an arbitrary unit of length, not to be confused with the spatial extent L. Red densities belong to patterns with characteristic length scale 2.0 [L], but same regularity as the blue patterns. The maxima S_{xc}^+ of patterns with the same regularity is not identical when their length scale differs. (b) After scaling distance by $1/\lambda_c$, the maximum of the density occurs at the rescaled wavenumber $k/k_c = 1$. The maximum $S_{xc}^+/\lambda_c = S_{xc}^+ \cdot k_c/(2\pi)$ of the rescaled density is a length-scale independent measure of the regularity, i.e. patterns with same regularity have the same rescaled maximum, independently of their characteristic length scale.

Where S_{xc} and S_{yc} are the maxima of the one-dimensional component in the direction perpendicular and parallel to the stripes, respectively. The definition also applies to rare cases where the pattern oscillates in the direction perpendicular to the stripes, referred to as dashed, pearled, or rhombic patterns (Siero et al., 2015). In this case the maximum S_{yc} occurs at the wavenumber $k_{yc} > 0$ so that the pattern has a second length-scale $\lambda_{yc} = 2\pi/k_{yc}$.

The regularity of an anisotropic pattern is anisotropic when the regularity in the two directions differs:

$$\text{Anisotropy of regularity} = \frac{S_{yc}}{S_{xc}^+}. \tag{10}$$

The contours of the density are circular, when the logarithm of the anisotropy is 0, i.e. when $S_{xc}^+ = S_{yc}$, and eccentric ellipses, when $S_{xc}^+ \ll S_{yc}$ or $S_{xc}^+ \gg S_{yc}$, , c.f. Fig. 5c. Striped patterns with the same regularity appear visually different when their anisotropies do not have the same value, c.f. Fig. 5d.

In polar coordinates, the two-dimensional regularity is:

$$\text{Regularity}_{r\theta} = 2\frac{S_{r\theta c}}{\lambda_c^2}. \tag{11a}$$

The regularity of an isotropic pattern is approximately equal to the product of the regularity in the radial and angular direction:

$$\text{Regularity}_{r\theta} \approx 2\,S_{\theta c}\frac{S_{rc}}{\lambda_c} = S_{\theta c}^+\frac{S_{rc}}{\lambda_c} \tag{11b}$$

Isotropic patterns appear the more regular, the larger the larger this value, c.f. Fig. 6c. S_{rc} and $S_{\theta c}$ are the maxima of the radial and angular density, respectively. This approximation is applicable to all types of isotropic patterns, i.e. to spotted, labyrinthine as well as gapped patterns. This is because the regularity is a property of the spatial structure, while the isotropic pattern type is primarily determined by the mean biomass.

For natural patterns where the spots or gaps are not aligned in a regular grid, the density is isotropic and the angular density uniform (flat), i.e. $S_\theta = (2\pi)^{-1}$ so the regularity is:

$$\text{Regularity}_{r\theta} \approx \frac{1}{\pi}\frac{S_{rc}}{\lambda_c}. \tag{11c}$$

The angular density S_θ for natural patterns is usually close to uniform, i.e. $S_{\theta c}^+ \approx \pi^{-1}$, even when the pattern is fairly regular along the radial direction.

The definition of the regularity in cartesian and polar coordinates are identical, i.e. $2\,S_{r\theta c}/\lambda_c^2 = 2\,S_{xyc}/\lambda_c^2$, as the transformation preserves the maximum. However, the approximation of the regularity based on the density composition is not identical, i.e. $S_{tc}^+\,S_{rc}/\lambda_c \neq S_{xc}^+\,\S_{yc}/\lambda_c^2$, due to the residual of the compositions. In general, only the approximation for the respective pattern type will be accurate.

2.5. Estimation of the regularity

The density is unknown for natural patterns and has to be estimated, typically from satellite images. We first demarcate the spatial extent of a pattern with a polygon and then crop the image to the bounding box of the polygon. The cropped satellite image has the rectangular spatial extent $L_x \times L_y$ consisting of $n_x \times n_y$ equispaced pixels. We derive

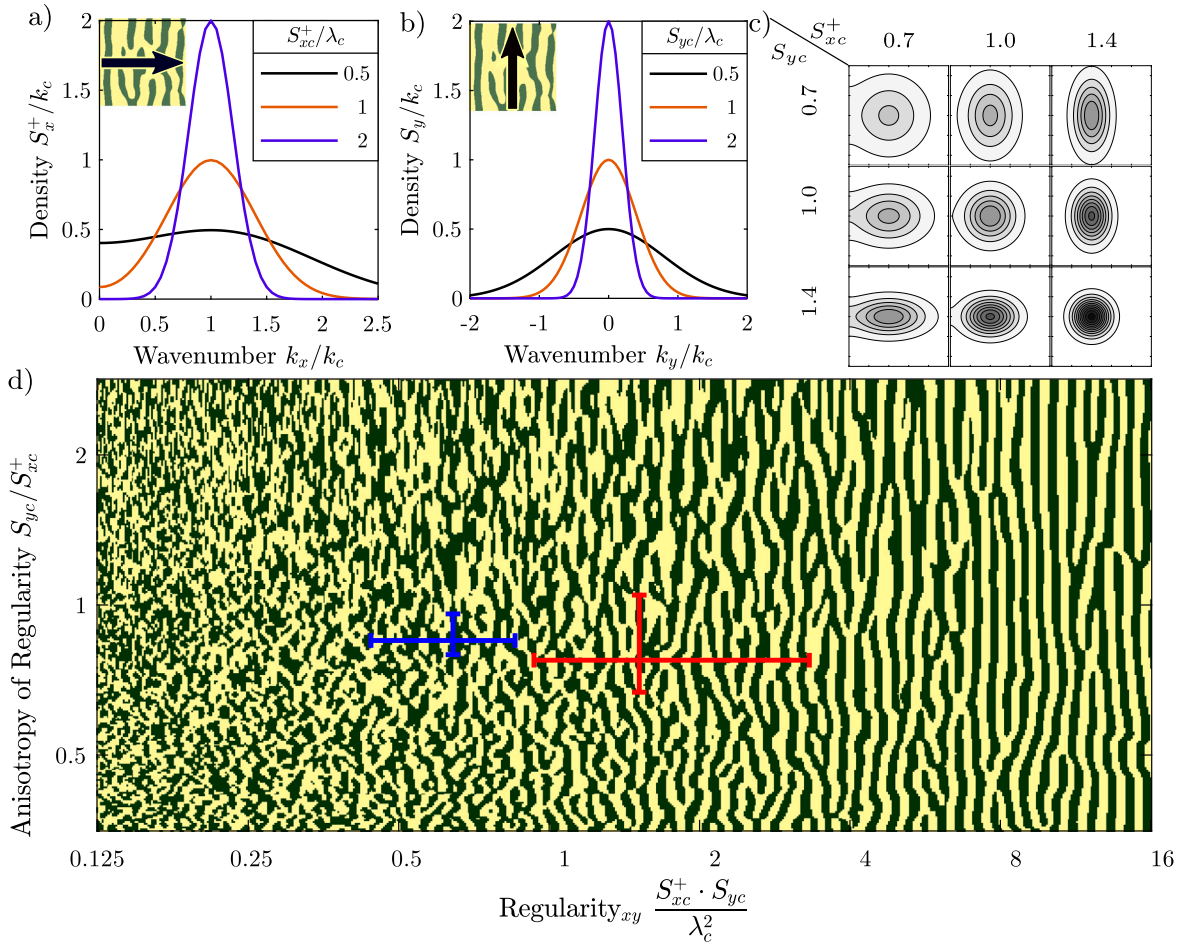

Fig. 5. Schematic spectral components of anisotropic patterns with different regularity in the direction (a) perpendicular to the stripes S_{xc}^+/λ_c and (b) parallel to the stripes S_{yc}/λ_c, when the density follows a bimodal bivariate normal distribution. (c) Two dimensional density S_{xy} for various combinations of S_{xc}^+/λ_c and S_{yc}/λ_c. Axis limits are $0 < k_x/k_c < 2.5, -1.25 < k_y/k_c < 1.25$. (d) Synthesized anisotropic pattern where the regularity $S_{xc} \cdot S_{yc}/\lambda_c^2$ increases from left to right and the anisotropy of the regularity S_{yc}/S_{xc} increases from the bottom to the top. The blue cross indicates the interquartile range of the estimated regularity of natural anisotropic patterns and the red cross the interquartile range of the estimated regularity of anisotropic model-generated patterns included in the metastudy, c.f. Fig. 7. The pattern has a bivariate bimodal normal density with varying regularity and was synthesized with a non-stationary stochastic process, c.f. supplement, section 1.16.

a proxy for the biomass concentration from the image and store it in the rectangular matrix B. We then compute the two-dimensional periodogram $\hat{S}_{xy}$ of the pattern as Kästner et al. (2024):

$$\hat{S}_{xy} = \frac{L_x\, L_y}{n_M^2\, \sigma_M^2} \left| \left(F_x \, \left(M \cdot \left(B - \mu_M \right) \right) \, F_y^T \right) \right|^2 \tag{12}$$

where $F_{x,ij} = \exp(-\mathrm{i}\, k_{xi}\, x_j)$ and $F_{y,ij} = \exp(-\mathrm{i}\, k_{yi}\, x_j)$ are the square Fourier matrices transforming columns and rows, respectively, with $x_i = L_x\, i/n_x$, $k_{xi} = 2\pi\, i/L_x$, $y_i = L_y\, i/n_y$, $k_{yi} = 2\pi\, i/L_y$. M is a matrix of the same size as B masking the area of patterns with arbitrary spatial extent. M has the value 1 in the pattern and 0 outside of the pattern. n_M is the number of pixels in the masked area, i.e. $n_M = n_x\, n_y$ when M fills the entire image. μ_M is the average and σ_M^2 the variance of B in the masked area. $\cdot$ denotes the element-wise product.

While the periodogram is the discrete analogue of the spectral density, it does not consistently estimate it, as its values randomly scatter, irrespectively how large the spatial extent or how fine the spatial resolution. We therefore estimate the regularity based on the axial averages of the histogram, which consistently estimate the density. For anisotropic patterns, we first rotate the periodogram so that the maximum of the density falls onto the x-axis, i.e. so that the stripes are on average perpendicular to the x-axis. We then integrate the periodogram in the respectively orthogonal direction to estimate the component in the direction perpendicular to the stripes $\bar{S}_{x,i} = \frac{\Delta k_y}{2\pi} \sum_j \hat{S}_{xy,ij}$, and the component parallel to the stripes $\bar{S}_{y,j} = \frac{\Delta k_x}{2\pi} \sum_i \hat{S}_{xy,ij}$. For isotropic patterns, we first transform the periodogram into polar coordinates and then estimate the radial density S_r as the integral of the two-dimensional density along angles for a particular radius, i.e. $\bar{S}_{r,i} = I_r\, \Delta\theta \sum_j S_{r\theta,ij}$, and the angular density by integrating along the radial direction for a particular angle, i.e. $\bar{S}_{\theta,j} = \frac{\Delta k_r}{(2\pi)^2} \sum_i k_{r,i} S_{r\theta,i}$.

Most natural patterns contain spurious low frequency components (Couteron, 2002). These are usually unrelated to the spatial structure of the pattern and originate for example from trends in soil reflectance. They appear as a second lobe centred at the origin $k = 0$ in the spectral density, beside the lobe of the regular spatial structure centred at the characteristic wavenumber k_c. We suppress this lobe with a high-pass filter before estimating the regularity. We determine the cut-off wavenumber of the filter as the wavenumber where the radial spectral density reaches its minimum between the maximum of the spurious lobe located at the origin and the maximum of the lobe of the regular structure, centred at the characteristic wavenumber, c.f. supplement, section 1.11. In the case the spatial extent of the masked pattern is elongated, i.e. when the effective side length differ, we smooth the density along the longer side to consistently estimate the density, c.f. supplement, section 1.10.

2.5.1. Uncertainty of the density estimate

The density estimates $\bar{S}_x, \bar{S}_y, \bar{S}_r$ and $\bar{S}_\theta$ have a random error, as they are averages of the randomly scattered periodogram. The error of the density estimate propagates to the regularity estimate. The error

depends both on the regularity of a pattern and the shape of the spectral density. The larger the relative spatial extent $L_x L_y/\lambda_c^2$, the smaller the error. The spatial extent of an image has therefore to be sufficiently large for reliably estimating the regularity. We recommend that the side length L spans at least ten wavelengths λ_c. For model-generated patterns, the regularity can be accurately estimated by making the computational domain sufficiently large. The spatial extent of most natural patterns is not large. The regularity of an individual pattern can therefore not be accurately estimated. The regularity should thus be evaluated as an ensemble for a particular regional, where the estimated regularity is combined into a more accurate estimate, for example into the median regularity. We elaborate on the uncertainty and how it is influenced by the spatial extent in detail in the supplement, section 1.12.

2.5.2. Bias of the regularity estimate

The regularity estimate is also biased, i.e. the error contains a systematic component. The bias propagates from the bias of the estimated maximum S_c and the characteristic wavenumber k_c of the mode. The maximum S_c is typically overestimated, especially for patterns with low regularity, as S_x is close to S_c in a wider wavenumber range so that it is likely that one of the values of $\bar{S}_x$ in this range, which randomly vary as described above, exceed the value S_{xc}. The bias of the characteristic wavenumber depends on the shape of the density. The characteristic wavenumber is typically underestimated, when the density is skewed towards low wavenumbers, as it is more likely that the maximum value of S_x occurs at wavenumbers lower than k_c but overestimated when the spectral density is skewed towards high wavenumbers. The spectral density is skewed towards high wavenumber, when it is log-normal and skewed towards low wavenumbers when S_x is (bimodal) normal so that the tails of the two modes at $\pm k_c$ add for low wavenumbers. It is therefore necessary to evaluate the shape of the density for estimating the bias, or even just its sign. When the regularity of the pattern is low, both the random error and the bias can be reduced by smoothing the density estimate $\bar{S}_x$ and $\bar{S}_r$. However, when the regularity of the pattern is high, smoothing increases the error as it reduces the height of the peak (Percival et al., 1993; Buttkus, 2010; Brillinger, 2001). The optimal degree of smoothing depends on the masked area, the regularity of the pattern, and the shape of the density. There is an optimal degree of smoothing for which the standard error is minimal. The uncertainty can also be reduced by fitting a parametric density. However, this estimate is also biased when the shape of the parametric density is not identical to that of the density of the pattern. Here, we do not apply a correction for reducing the bias or random error, as it is difficult to determine the optimal degree of smoothing or an appropriate density model, in particular if the spatial extent is not square but determined by masking.

2.5.3. Upper limit of the regularity estimate

For a pattern with finite spatial extent, the product $S_{xc}\,\Delta k/(2\pi) = S_{xc}/L_x$ is the fraction of spatial variation contributed by the main frequency component. For periodic patterns without harmonic frequency components, all the spatial variation stems from the dominant frequency component and the product is 1. A finite spatial extent consequently limits the maximum value that can be estimated for the regularity. For example, the regularity in the direction perpendicular to the bands can be at most L_x/λ_c, for anisotropic periodic patterns with a single frequency component. This can be understood by interpreting the regularity as the number of times a pattern repeats before decorrelating. When the spatial extent is finite, the maximum number of times a pattern can repeat is L_x/λ_c times. The estimated regularity for a cropped periodic pattern thus depends on the size of the spatial extent. For natural patterns, the estimated regularity does not depend on the spatial extent, as the regularity is typically smaller than the limit set by the spatial extent (see Fig. 6).

3. Meta-analysis of regular environmental spatial patterns

To gauge the regularity of environmental spatial patterns and to determine how well computer models reproduce it, we conduct a systematic study on spatial patterns displayed in the literature. We include 238 patterns displayed in the literature and in this very publication. The patterns are selected from the 60 most cited and recent publications which display regular environmental spatial patterns. A detailed list of references with analysis results is given in the supplement, section 2.

We only include patterns where the length scale can be clearly identified, i.e. exclude scale-free patterns. We manually extracted the images with patterns from the publications, including only clearly regular patterns, i.e. patterns where the spectral density consists of a lobe where the mode is well separated from the origin. As we only include highly regular patterns in the study, the cut-off wavenumber for the suppression of low-frequency components is well defined. We also include only natural patterns or patterns generated by models which mimic environmental systems, i.e. exclude schematic figures. Most model-generated patterns displayed in the literature have been generated with deterministic models. A few patterns though have been generated with models which incorporate stochasticity. We analyse them separately. For publications which display many patterns, we select a representative subset, to avoid bias towards those publications.

We prepare the images by manually cropping away frames and specifying masks to exclude annotations and areas surrounding natural patterns, and grouped them into natural and model-generated patterns, as well as into one-dimensional and two-dimensional patterns. The remainder of the processing is automatic, including the classification as isotropic and anisotropic patterns, the suppression of spurious low frequency components, c.f. supplement section 1.11, the periodicity test Kästner et al. (2024) and the estimation of the regularity. We use order statistics for the analysis of the regularities, as they are robust against outliers and deviation from normality. We present the median and quartiles for the regularity of natural and computer generated patterns, and test for a difference between the medians of the groups (Mood, 1954). We used Kendall's correlation, retransformed to Pearson's measure (Kruskal, 1958), to explore the relation between the regularity in the two principal directions, x-y and r-s, respectively.

Measured along the primary axis, i.e. in the direction perpendicular to the stripes, anisotropic natural patterns have a median regularity S_{xc}/λ_c of 0.80 compared to 1.93 for patterns generated with deterministic two-dimensional models, and 3.52 for patterns generated with one-dimensional models (Fig. 8a). Along the radial direction, natural isotropic patterns have a median regularity S_{rc}/λ_c of 0.67 compared to 2.36 for patterns generated with deterministic models. The differences between the median regularity along the primary axis of natural patterns and patterns generated with two-dimensional deterministic models are highly significant, with Mood's median test yielding $p = 3.5 \cdot 10^{-08}$ for anisotropic and $8.9 \cdot 10^{-12}$ for isotropic patterns. Studies using stochastic models are rare, with no study on anisotropic patterns and only a few studies on isotropic patterns. The regularity of isotropic patterns generated with stochastic models is closer to that of the natural ones with a regularity S_{xc}/λ_c of 1.18 (Fig. 8b). Patterns with lower regularity can of course also be generated with models which do not incorporate scale dependent feedbacks, for example, the isotropic patterns in Siteur et al. (2023) have a median regularity of 1.40 on the radial direction.

The contrast is also strong for anisotropic patterns along the secondary axis. For anisotropic patterns, the median regularity in the direction parallel to the stripes S_{yc}/λ_c is 0.53 for natural and 1.15 for model-generated patterns (Fig. 8c). For isotropic patterns, the difference is smaller, with a median regularity along the angular-axis $S_{c,\theta}$ is 0.42 for natural and 0.51 for computer generated patterns, respectively (Fig. 8d). The analysis thus confirms that the regularity of model-generated patterns is systematically higher than that of natural patterns.

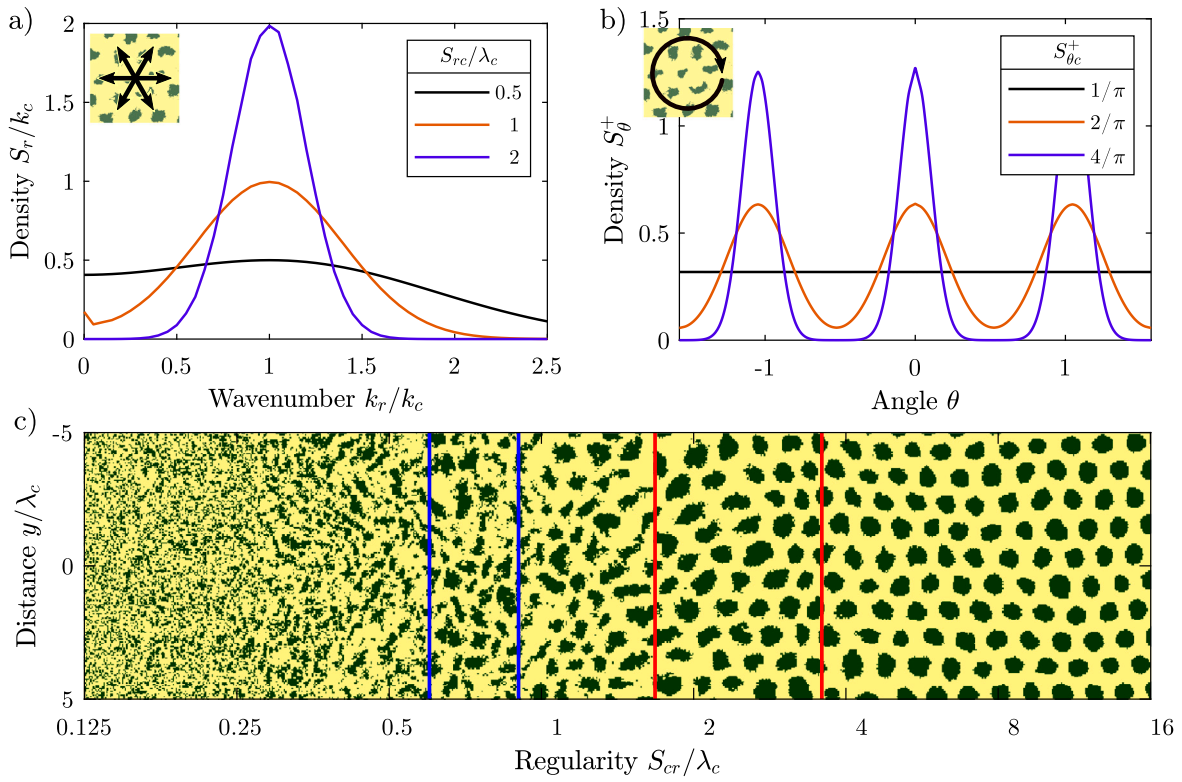

Fig. 6. Schematic (a) radial and (b) angular spectral component of isotropic patterns. (c) Synthesized isotropic pattern where the regularity S_{rc}/λ_c increases from left to right. Red and blue vertical lines indicate the interquartile ranges of natural and model-generated patterns, c.f. Fig. 7. Pattern synthesized with a non-stationary stochastic process, c.f. supplement, section 1.16.

For anisotropic patterns, the correlation between the regularity in the direction perpendicular (S_{xc}/λ_c) and parallel (S_{yc}/λ_c) to stripes was very high, with 0.998 for natural and 0.897 for model-generated patterns. Due to the high correlation, the regularity as a whole can be reasonably assessed by the regularity in the direction perpendicular to the stripes. For isotropic patterns, the correlation between the radial S_r/λ_c and angular S_s/λ_c regularity is low for natural patterns (−0.258) but high for model generated patterns (0.971). This difference is not coincidental, because natural patterns tend to be stochastic with a uniform angular density so that the regularity is primarily determined by the radial density. The model-generated patterns tend to form a periodic hexagonal pattern in contrast, where the maxima of both the radial and angular density is primarily determined by the pattern size L. The spatial structure of model-generated patterns thus systematically differs from the natural ones.

The systematic overprediction of the regularity by model-generated patterns is also corroborated by the periodicity test of Kästner et al. (2024). Only 10% of the natural patterns in the metastudy have significant frequency components at a confidence level of $p = 0.05$, not too far from the 5% expected by chance, while 53% of the patterns generated with non-stochastic models in the metastudy pass the periodicity test. Model generated patterns thus tend to be periodic, while natural patterns do not.

3.1. Spectral densities

This difference between the model-generated and natural patterns becomes apparent when comparing their spectral densities. Along the primary axis, the rescaled density S_x/λ_c, or respectively S_r/λ_c, of the model-generated patterns is on average much narrower and higher than that of the natural patterns (Fig. 8a,c). The same holds for the rescaled density S_y/λ_c of anisotropic patterns in the direction parallel to the stripes (Fig. 8b). The angular density S_θ of model-generated patterns consists of six peaks as expected for hexagonal patterns, while the angular density of natural patterns is essentially flat (Fig. 8d). The model-generated patterns are therefore considerably more regular than natural patterns.

We note that the regularity of the average density S_x^+ and S_r is identical to the average regularity of the patterns, though the averaging introduces several distortions. Parametric density models should thus not be chosen based on the shape of the average density. However, this does not influence the comparison of model-generated patterns with natural patterns, as the artefacts distort both groups in a similar manner. Averaging distorts the shape of the densities along the primary axis S_x^+ and S_y, increasing its kurtosis so that the is the peak of the averaged density is more pointed and the tail heavier compared to the density of a single pattern, which can be visualized by averaging two Gaussian densities with the same mean but different standard deviation: the average density is as sharply pointed as the density with the lower standard deviation near the mean, but has similar tails as the density with the higher standard deviation, c.f. illustration in the supplement, section 1.13. Another artefact is introduced by rotating the densities before averaging so that their maximum occurs at the angle $\theta = 0$, as this exaggerates the peak of the angular density S_θ at the origin (Fig. 8d).

The regularity varies strongly within each group in the dataset of our metastudy, as patterns stem from very different ecosystems and are generated with different models, as evident from the interquartile ranges in Fig. 7. However, the overprediction of regularity by modelled patterns is nonetheless very clear. Several factors make us believe that the contrast between natural and model-generated patterns might be even stronger than indicated by the metastudy. First, the regularity of the model-generated patterns in the metastudy is likely underestimated, as the spatial extent of most model-generated patterns in the metastudy is relatively small, with a median of 7 characteristic wavelengths only. The regularity of the natural patterns in contrast is not strongly affected

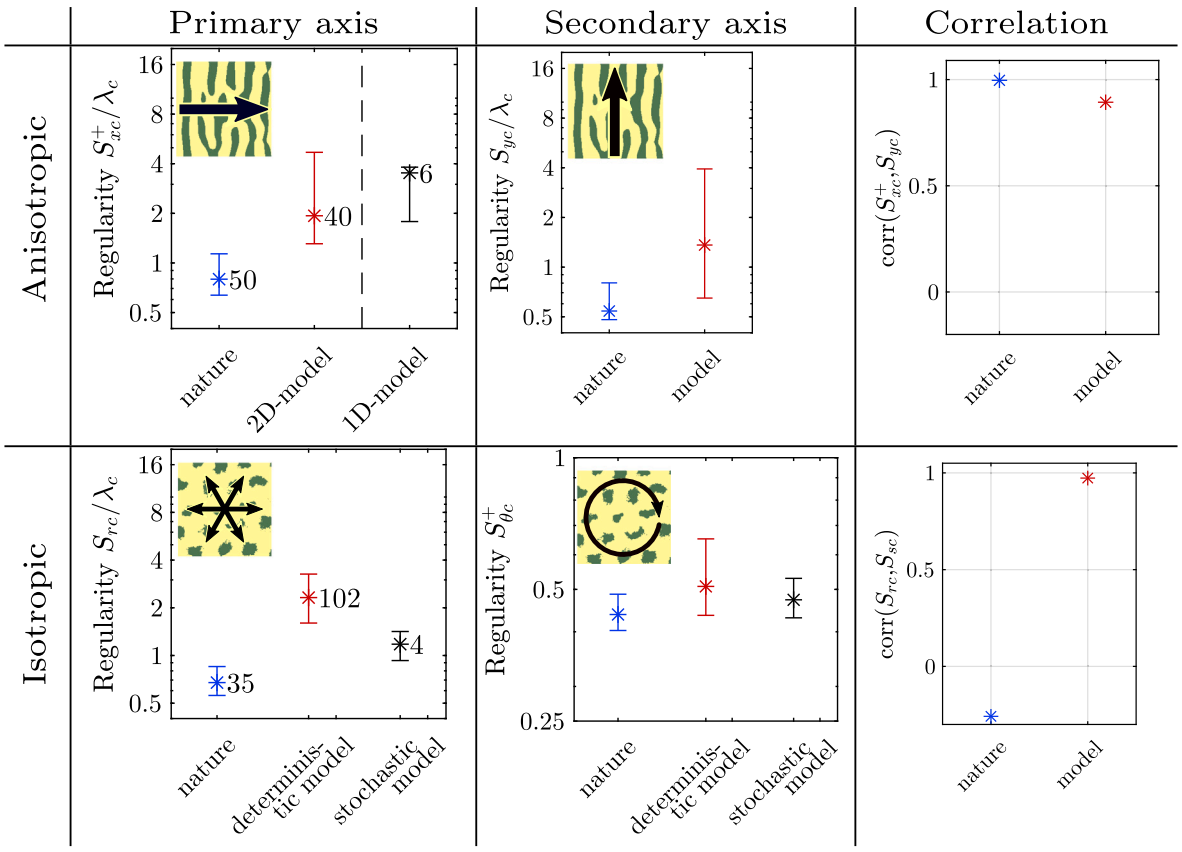

Fig. 7. Regularity of patterns included in the meta-analysis. The stars indicate the median, sticks the interquartile range. Numbers are the number of samples within each group. There are no anisotropic patterns generated with stochastic models in the dataset. Note that the interquartile range indicates the variation in the data, not the uncertainty in the median, which is smaller. We provide a complementary figure with confidence intervals in the supplement, Fig. 11.

by their spatial extent, as it is sufficiently large, with a median of 11 characteristic wavelengths, when accounted for masking. Second, it is plausible that the regularity of natural patterns is overestimated, as it is likely that studies preferentially display natural patterns, or parts thereof, which appear particularly regular.

4. Discussion and conclusion

Conventionally, spatial patterns have been classified as being either regular or irregular, and the spatial structure of regular patterns has been primarily characterized by their dominant wavelength. Here, we find that regularity is a nuanced property which can take any state in between the limit cases of an irregular or a periodic spatial structure. At least two parameters are required for describing the spatial structure of regular patterns, one for its characteristic length scale and one for its regularity. As the spatial structure of patterns is primarily determined by their spectral density, the two parameters are derived from the characteristic wavelength and the degree of variation around it. How regular a pattern appears depends on how closely the spectral energy is concentrated around its dominant frequency component. Based on this observation, we introduce a method for quantifying the degree of regularity of environmental spatial patterns, beyond the binary classification of regular patterns as regular or not. Our method is based on the height of the mode of the rescaled density and yields a value in between the extreme limits of irregular pattern with no finite characteristic length scale and periodic patterns, where all the spatial variation is explained by the characteristic frequency component and its harmonics. Our method allows one to compare the spatial structure quantitatively, for example between field sites or for validating models. Our approach is in line with recent recommendations that discourage the use of statistical tests with dichotomous outcomes (Cumming, 2014; Wasserstein and Lazar, 2016), and calls for embracing variation in data (Gelman and Carlin, 2017) and for adopting more holistic approaches beyond significance testing (Wasserstein et al., 2019).

We advocate for our regularity measure based on the height of the mode, as it is simple and can be directly read from a plot of the rescaled spectral density. It is uniquely defined, can distinguish between irregular and regular patterns, and is relatively insensitive to the shape and the tails of the distribution of the spectral density, as well as only moderately sensitive to the uncertainty of the density estimate it is based on. The regularity measure can also be based on various other properties of a pattern, such as the width of mode, the interquartile range, the standard deviation, or the entropy of the spectral density, the decay rate of the autocorrelation, as well as various statistics of patch sizes and spacing. We compare the alternatives in detail in the supplement, section 1.15, and show that the measures based on the spectral density and autocorrelation can be uniquely transformed into comparable values when the particular distribution type of the spectral density is known and the value of the property is finite. The transformed measures further converge to the same limit with increasing regularity of a pattern. For an unknown distribution, the transformed values differ at most by a constant factor for sufficiently regular patterns. While equivalent for highly regular patterns, the reliability of the methods differs in the general case. The standard deviation of the density is not a suitable property for measuring, as it is sensitive to the tails and not finite for several common unimodal distributions, including distributions of binarized patterns. The entropy is also sensitive to tails. Measures based on the autocorrelation suffer from ambiguity in detecting the oscillation corresponding to the characteristic component when harmonic frequency components are present. The estimates based on the width of the mode is close to the estimate based on the height of the mode, but complications arise when

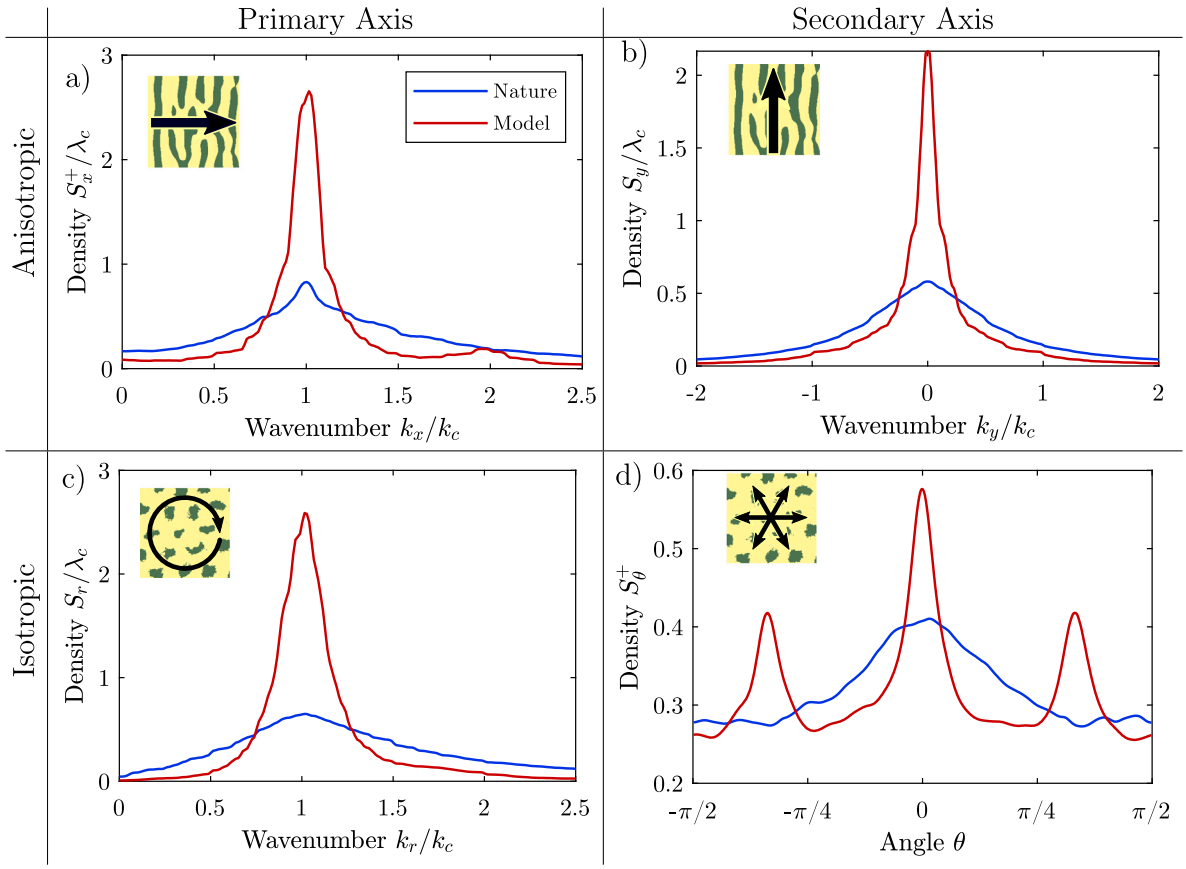

Fig. 8. Averaged spectral densities of anisotropic patterns in the direction (a) perpendicular to stripes and (c) parallel to stripes, and for isotropic patterns (b) along radii and (d) along concentric rings, averaged over all patterns within the respective group, separated into natural (blue) and model-generated (red) patterns. We rescale the spectral densities before averaging so that the maximum of all patterns occurs at $k_c'/(2\pi) = 1$. Spurious low frequency components with wavenumbers $k \ll k_c$ have been suppressed in the periodogram before computing the densities, c.f. Fig. 4. Note that regularity of the average primary densities S_x and S_r is the same as the average regularity of the individual patterns, but the shape of the density becomes more pointed near the maximum due to the averaging. The maximum of the angular density S_θ^+ at the origin is overestimated, as we rotate the maximum to 0 before averaging.

the regularity is low, as the modes on the positive and negative half-plane merge. It is also more sensitive to the uncertainty in the density estimate. Comparable transformations for statistics of the patch size and spacing can probably be found for patterns that are sufficiently regular. We do not explore patch statistics further, as they are local properties and hence unsuitable for distinguishing patterns with intermediate regularity from patterns with periodic spatial structure in the general case (Kästner et al., 2024). However, patch statistics can be favourable for studying the variation of local properties of patterns, such as along hillslopes (Pinto-Ramos et al., 2023). They are also affected by the ambiguity in the identification of individual patches

4.1. Regularity of environmental spatial patterns

Our metastudy reveals that environmental spatial patterns are of intermediate regularity. Their spectral energy is scattered over a wide frequency range, in proportion to a lobed spectral density which is typical for random fields generated by stochastic processes (Yaglom, 1962; Percival et al., 1993; Buttkus, 2010; Lindgren et al., 2013). This differs from periodic patterns where the spectral energy is concentrated in well-separated narrow peaks. While the number of patterns in the metastudy is moderate (≈ 200), and estimates of regularity inevitably depend how patterns are identified as such and how their spatial extent is delineated, the overall finding that environmental spatial patterns are of intermediate regularity is in agreement with our recent study where we test a much larger number (≈ 10 000) of regular environmental spatial patterns for periodicity (Kästner et al., 2024). Our finding contradicts the established view of regular environmental spatial patterns as periodic (Meron, 2015). However, the intermediate regularity of natural patterns and correspondingly the scattering of the spectral energy over a relatively wide frequency range, is hidden in plain sight in many publications without that this was recognized in those publications (Lejeune et al., 1999; Couteron, 2001; Couteron and Lejeune, 2001; Couteron, 2002; van de Koppel et al., 2005; van de Koppel and Crain, 2006; Barbier et al., 2006; Koffi et al., 2008; Wang et al., 2009; Deblauwe et al., 2011; Kefi et al., 2014; Couteron et al., 2014; Tarnita et al., 2017). While the distinction between periodic and regular is a mathematical formality, it is relevant for the conceptual understanding of pattern forming ecosystems, since conventional models generate patterns which are considerably more regular than natural ones. Our metastudy reveals that patterns generated with deterministic models are indeed much more regular than natural ones. Conclusions drawn from these models are not necessarily invalid. However, since the spatial structure is frequently employed as an indicator of ecosystem health and resilience, caution is warranted.

Our metastudy also reveals that patches in natural isotropic patterns are aligned randomly and not in a hexagonal grid as patterns generated with deterministic models. While patches in natural regular patterns are typically surrounded by six neighbours, the angle of rotation varies locally. The angular spectral density of natural isotropic patterns is consequently flat, in contrast to the discrete density with six peaks of patterns generated with deterministic models. The patches in natural patterns do not align in a grid, as there is no process which imposes a direction. Patches probably align with respect to local exogenous perturbations. The gridded hexagonal structure of model-generated patterns is thus likely an artefact of homogeneous model domains. This is

different in anisotropic systems, where natural processes indeed impose globally a direction. Vegetation at hillslopes, for example, aligns parallel to the elevation contours as water flows downhill. The difference in the spatial structure of natural isotropic and hexagonal model-generated patterns can be revealed by estimating the spectral density by first splitting a pattern into tiles of equal size and than averaging the periodograms of the tiles Bartlett (1948): while patches in natural patterns have on average six neighbours, the axes of rotation vary between the tiles, so that the peaks in the periodograms of the individual tiles do not constructively overlap during averaging which results in a flat angular density. In contrast, patches are aligned globally along the same axes in model-generated patterns so that the peaks in the angular spectrum overlap which results in an angular density with six peaks. The same result can also be reached by determining local directions based on a Voronoi tessellation around patch centres (Bordeu et al., 2016). While the hexagonal structure of model-generated structures is typically imperfect, it is polychrystalline, i.e. it consists of regions with hexagonal structures, which are separated by sharp boundaries and differ in their rotational angle. This spatial structure is reflected in their radial spectrum consisting of a narrow and high peak, which is still quite different to the lobed density of natural regular patterns.

4.2. Causes of intermediate regularity

A possible reason for the lower regularity of natural patterns could be the influence of processes without scale-dependent feedbacks on the pattern formation. For example, vegetation patterns can form by the attraction of grazers to areas with young grass and respectively low biomass, rather than by the redistribution of water (Siteur et al., 2023). However, while this can be a factor in savannahs, it cannot explain the lower regularity of patterns in semi-arid regions where patches of biomass are separated by bare ground. Pinto-Ramos et al. (2023) showed that striped patterns with intermediate regularity can form under certain conditions due to instabilities at the boundary. However, this still predicts periodic patterns for a wide parameter range, and thus cannot explain the general absence of periodic striped patterns (Kästner et al., 2024). It also cannot explain the lack of periodicity of isotropic patterns. Another possible explanation could be that the spatial structure of natural patterns is still in a transient state, i.e. they are still strongly influenced by a random initial condition and yet have to crystallize into periodic structure. However, while the initial condition can influence the spatial patterns for long times, even indefinitely (Caviedes-Voullième and Hinz, 2020), model-generated patterns appear much more regular than natural patterns after relatively short periods, i.e. a couple of decades. A plausible explanation for the intermediate regularity is that regular patterns form through stochastic processes, i.e. through random spatial perturbation to the biophysical processes (van Kampen, 1976), which can be reconciled with established models, as deterministic models can be made stochastic by slightly varying the model coefficients in space. A few studies incorporated spatial noise in their models and generated less regular patterns (Thompson et al., 2008; McGrath et al., 2012; Yizhaq et al., 2014; Yizhaq and Bel, 2016; Yizhaq et al., 2017; Echeverría-Alar et al., 2023). However, the means by which spatial heterogeneities modulate the pattern formation has not yet been explored. Further research is also necessary to study the sources of environmental heterogeneity, their magnitude and scales. Potential factors are soil properties (Baveye and Laba, 2015), in particular grain size, modulating infiltration and plant growth, topography (van der Ploeg et al., 2012; McGrath et al., 2012; Caviedes-Voullième et al., 2021), modulating the flow of water, as well as biotic factors, such as seed dispersal (Consolo and Valenti, 2019) and localized faunal activity (Eldridge et al., 2012). Random environmental heterogeneities should be put in context with the more easily recognizable systematic variations in the environment, for example along catenas (Nicolau et al., 1996) or across valleys (Gandhi et al., 2018). Another possible factor is spatially random faunal activity.

The response of regular environmental spatial patterns to environmental pressure, such as overgrazing or declining precipitation due to climate change has predominantly been studied with deterministic models generating periodic patterns (Kealy and Wollkind, 2012; van der Stelt et al., 2013; Sherratt, 2013; Siteur et al., 2014b,a; Kyriazopoulos et al., 2014; Kinast et al., 2014; Dagbovie and Sherratt, 2014; Zelnik et al., 2016; Sherratt and Mackenzie, 2016; Gowda et al., 2016; Zelnik et al., 2017, 2018). It remains to be studied to what extent heterogeneity matters for ecosystem resilience and productivity. Environmental heterogeneity likely matters because a pattern with intermediate regularity will respond slightly differently in distinct location to environmental pressure, due to its finite correlation length, while a periodic pattern can only adapt in its entirety, thereby facilitating catastrophic shifts like the simultaneous die back of either all vegetation patches or of every other patch. Our method can reliably quantify spatial regularity, which is essential for unravelling the relations between a pattern's structure and the ecosystem's productivity and resilience.

CRediT authorship contribution statement

Karl Kästner: Conceptualization, Formal analysis, Investigation, Methodology, Software, Writing – original draft, Writing – review & editing, Data curation. **Roeland C. van de Vijsel:** Writing – review & editing. **Daniel Caviedes-Voullième:** Writing – review & editing. **Christoph Hinz:** Writing – review & editing.

Declaration of competing interest

The authors declare that they have no known competing financial interests or personal relationships that could have appeared to influence the work reported in this paper.

Appendix A. Supplementary data

Supplementary material related to this article can be found online at https://doi.org/10.1016/j.ecocom.2024.101104.

Data availability

Scripts for the analysis and numerical modelling of vegetation patterns are available at https://github.com/karlkastner/environmental-spatial-patterns-metastudy. An archive containing the source code including dependencies is available at Zenodo: https://zenodo.org/records/13974157.

References

Barbier, N., Couteron, P., Lejoly, J., Deblauwe, V., Lejeune, O., 2006. Self-organized vegetation patterning as a fingerprint of climate and human impact on semi-arid ecosystems. J. Ecol. 94 (3), 537–547.

Bartlett, M.S., 1948. Smoothing periodograms from time-series with continuous spectra. Nature 161 (4096), 686–687.

Bastiaansen, R., Doelman, A., Eppinga, M.B., Rietkerk, M., 2020. The effect of climate change on the resilience of ecosystems with adaptive spatial pattern formation. Ecol. Lett. 23 (3), 414–429.

Bastiaansen, R., Jaïbi, O., Deblauwe, V., Eppinga, M.B., Siteur, K., Siero, E., Mermoz, S., Bouvet, A., Doelman, A., Rietkerk, M., 2018. Multistability of model and real dryland ecosystems through spatial self-organization. Proc. Natl. Acad. Sci. 115 (44), 11, 256–11, 261.

Baveye, P.C., Laba, M., 2015. Moving away from the geostatistical lamppost: Why, where, and how does the spatial heterogeneity of soils matter? Ecol. Model. 298, 24–38.

Bel, G., Hagberg, A., Meron, E., 2012. Gradual regime shifts in spatially extended ecosystems. Theoret. Ecol. 5, 591–604.

Bennett, J.J., Gomes, A.S., Ferré, M.A., Bera, B.K., Borghetti, F., Callaway, R.M., Meron, E., 2023. Evidence for scale-dependent root-augmentation feedback and its role in halting the spread of a pantropical shrub into an endemic sedge. PNAS nexus 2 (1), pgac294.

Bera, B.K., Tzuk, O., Bennett, J.J., Meron, E., 2021. Linking spatial self-organization to community assembly and biodiversity. Elife 10, e73819.
Bonachela, J.A., Pringle, R.M., Sheffer, E., Coverdale, T.C., Guyton, J.A., Caylor, K.K., Levin, S.A., Tarnita, C.E., 2015. Termite mounds can increase the robustness of dryland ecosystems to climatic change. Science 347 (6222), 651–655.
Bordeu, I., Clerc, M.G., Couteron, P., Lefever, R., Tlidi, M., 2016. Self-replication of localized vegetation patches in scarce environments. Sci. Rep. 6 (1), 33703.
Borgogno, F., D'Odorico, P., Laio, F., Ridolfi, L., 2009. Mathematical models of vegetation pattern formation in ecohydrology. Rev. Geophys. 47 (1).
Brillinger, D.R., 2001. Time Series: Data Analysis and Theory. SIAM.
Buttkus, B., 2010. Spectral Analysis and Filter Theory in Applied Geophysics. Springer Science & Business Media.
Caviedes-Voullième, D., Ahmadinia, E., Hinz, C., 2021. Interactions of microtopography, slope and infiltration cause complex rainfall-runoff behavior at the hillslope scale for single rainfall events. Water Resour. Res. 57 (7), e2020WR028127.
Caviedes-Voullième, D., Hinz, C., 2020. From nonequilibrium initial conditions to steady dryland vegetation patterns: How trajectories matter. Ecohydrology 13 (3), e2199.
Clerc, M.G., Echeverría-Alar, S., Tlidi, M., 2021. Localised labyrinthine patterns in ecosystems. Sci. Rep. 11 (1), 18331.
Consolo, G., Valenti, G., 2019. Secondary seed dispersal in the Klausmeier model of vegetation for sloped semi-arid environments. Ecol. Model. 402, 66–75.
Cornacchia, L., van de Koppel, J., van der Wal, D., Wharton, G., Puijalon, S., Bouma, T.J., 2018. Landscapes of facilitation: how self-organized patchiness of aquatic macrophytes promotes diversity in streams. Ecology 99 (4), 832–847.
Couteron, P., 2001. Using spectral analysis to confront distributions of individual species with an overall periodic pattern in semi-arid vegetation. Plant Ecol. 156 (2), 229–243.
Couteron, P., 2002. Quantifying change in patterned semi-arid vegetation by Fourier analysis of digitized aerial photographs. Int. J. Remote Sens. 23 (17), 3407–3425.
Couteron, P., Hunke, P., Bellot, J., Estrany, J., Martínez-Carreras, N., Mueller, E.N., Papanastasis, V.P., Parmenter, R.R., Wainwright, J., 2014. Characterizing patterns. In: Patterns of Land Degradation in Drylands. Springer, pp. 211–245.
Couteron, P., Lejeune, O., 2001. Periodic spotted patterns in semi-arid vegetation explained by a propagation-inhibition model. J. Ecol. 89 (4), 616–628.
Cumming, G., 2014. The new statistics: Why and how. Psychol. Sci. 25 (1), 7–29.
Dagbovie, A.S., Sherratt, J.A., 2014. Pattern selection and hysteresis in the Rietkerk model for banded vegetation in semi-arid environments. J. R. Soc. Interface 11 (99), 20140465.
Dale, M.R., 2000. Spatial Pattern Analysis in Plant Ecology. Cambridge University Press.
Deblauwe, V., Couteron, P., Lejeune, O., Bogaert, J., Barbier, N., 2011. Environmental modulation of self-organized periodic vegetation patterns in Sudan. Ecography 34 (6), 990–1001.
Dunkerley, D.L., 1997. Banded vegetation: development under uniform rainfall from a simple cellular automaton model. Plant Ecol. 129, 103–111.
Echeverría-Alar, S., Pinto-Ramos, D., Tlidi, M., Clerc, M., 2023. Effect of heterogeneous environmental conditions on labyrinthine vegetation patterns. Phys. Rev. E 107 (5), 054219.
Eldridge, D.J., Koen, T.B., Killgore, A., Huang, N., Whitford, W.G., 2012. Animal foraging as a mechanism for sediment movement and soil nutrient development: evidence from the semi-arid Australian woodlands and the Chihuahuan Desert. Geomorphology 157, 131–141.
Fernandez-Oto, C., Tzuk, O., Meron, E., 2019. Front instabilities can reverse desertification. Phys. Rev. Lett. 122 (4), 048101.
Gandhi, P., Werner, L., Iams, S., Gowda, K., Silber, M., 2018. A topographic mechanism for arcing of dryland vegetation bands. J. R. Soc. Interface 15 (147), 20180508.
Gelman, A., Carlin, J., 2017. Some natural solutions to the *p*-value communication problem—and why they won't work. J. Amer. Statist. Assoc. 112 (519), 899–901.
Gilad, E., von Hardenberg, J., Provenzale, A., Shachak, M., Meron, E., 2007. A mathematical model of plants as ecosystem engineers. J. Theoret. Biol. 244 (4), 680–691.
Gowda, K., Chen, Y., Iams, S., Silber, M., 2016. Assessing the robustness of spatial pattern sequences in a dryland vegetation model. Proc. R. Soc. A: Math. Phys. Eng. Sci. 472 (2187), 20150893.
Hille Ris Lambers, R., Rietkerk, M., van den Bosch, F., Prins, H.H., de Kroon, H., 2001. Vegetation pattern formation in semi-arid grazing systems. Ecology 82 (1), 50–61.
Inderjit, Callaway, R.M., Meron, E., 2021. Belowground feedbacks as drivers of spatial self-organization and community assembly. Phys. Life Rev. 38, 1–24. http://dx.doi.org/10.1016/j.plrev.2021.07.002.
Kabir, M.H., Gani, M.O., 2022. Numerical bifurcation analysis and pattern formation in a minimal reaction–diffusion model for vegetation. J. Theoret. Biol. 536, 110997.
Kästner, K., van de Vijsel, R., Caviedes-Voullième, D., Frechen, N.T., Hinz, C., 2024. Unravelling the spatial structure of regular environmental spatial patterns. Catena (In press).
Kealy, B.J., Wollkind, D.J., 2012. A nonlinear stability analysis of vegetative turing pattern formation for an interaction–diffusion plant-surface water model system in an arid flat environment. Bull. Math. Biol. 74 (4), 803–833.
Kéfi, S., Eppinga, M.B., de Ruiter, P.C., Rietkerk, M., 2010. Bistability and regular spatial patterns in arid ecosystems. Theoret. Ecol. 3 (4), 257–269.
Kefi, S., Guttal, V., Brock, W.A., Carpenter, S.R., Ellison, A.M., Livina, V.N., Seekell, D.A., Scheffer, M., van Nes, E.H., Dakos, V., 2014. Early warning signals of ecological transitions: methods for spatial patterns. PLoS One 9 (3), e92097.
Kéfi, S., Rietkerk, M., Alados, C.L., Pueyo, Y., Papanastasis, V.P., ElAich, A., De Ruiter, P.C., 2007. Spatial vegetation patterns and imminent desertification in Mediterranean arid ecosystems. Nature 449 (7159), 213–217.
Kéfi, S., Rietkerk, M., Roy, M., Franc, A., De Ruiter, P.C., Pascual, M., 2011. Robust scaling in ecosystems and the meltdown of patch size distributions before extinction. Ecol. Lett. 14 (1), 29–35.
Kinast, S., Zelnik, Y.R., Bel, G., Meron, E., 2014. Interplay between Turing mechanisms can increase pattern diversity. Phys. Rev. Lett. 112 (7), 078701.
Klausmeier, C.A., 1999. Regular and irregular patterns in semiarid vegetation. Science 284 (5421), 1826–1828.
Koffi, K.J., Deblauwe, V., Sibomana, S., Neuba, D.F.R., Champluvier, D., Canniere, C.D., Barbier, N., Traore, D., Habonimana, B., Robbrecht, E., et al., 2008. Spatial pattern analysis as a focus of landscape ecology to support evaluation of human impact on landscapes and diversity. In: Landscape Ecological Applications in Man-Influenced Areas. Springer, pp. 7–32.
Kruskal, W.H., 1958. Ordinal measures of association. JASA 53 (284), 814–861.
Kyriazopoulos, P., Nathan, J., Meron, E., 2014. Species coexistence by front pinning. Ecol. Complex. 20, 271–281.
Lefever, R., Lejeune, O., 1997. On the origin of tiger bush. Bull. Math. Biol. 59 (2), 263–294.
Lejeune, O., Couteron, P., Lefever, R., 1999. Short range co-operativity competing with long range inhibition explains vegetation patterns. Acta Oecol. 20 (3), 171–183.
Lejeune, O., Tlidi, M., Lefever, R., 2004. Vegetation spots and stripes: Dissipative structures in arid landscapes. Int. J. Quant. Chem. 98 (2), 261–271.
Lindgren, G., Rootzén, H., Sandsten, M., 2013. Stationary stochastic processes theory and applications. In: Theory and Applications; Texts in Statistical Science Series. p. 347.
McGrath, G.S., Paik, K., Hinz, C., 2012. Microtopography alters self-organized vegetation patterns in water-limited ecosystems. J. Geophys. Res.: Biogeosci. 117 (G3).
Meron, E., 2015. Nonlinear Physics of Ecosystems. CRC Press, Boca Raton, FL.
Mood, A.M., 1954. On the asymptotic efficiency of certain nonparametric two-sample tests. Ann. Math. Stat. 514–522.
Nicolau, J., Solé-Benet, A., Puigdefábregas, J., Gutiérrez, L., 1996. Effects of soil and vegetation on runoff along a catena in semi-arid Spain. Geomorphology 14 (4), 297–309.
Percival, D.B., Walden, A.T., et al., 1993. Spectral Analysis for Physical Applications. cambridge University Press.
Pinto-Ramos, D., Clerc, M., Tlidi, M., 2023. Topological defects law for migrating banded vegetation patterns in arid climates. Sci. Adv. 9 (31), eadf6620.
Renshaw, E., Ford, E., 1984. The description of spatial pattern using two-dimensional spectral analysis. Vegetatio 56 (2), 75–85.
Rietkerk, M., Bastiaansen, R., Banerjee, S., van de Koppel, J., Baudena, M., Doelman, A., 2021. Evasion of tipping in complex systems through spatial pattern formation. Science 374 (6564), eabj0359.
Rietkerk, M., Boerlijst, M.C., van Langevelde, F., Hille Ris Lambers, R., van de Koppel, J., Kumar, L., Prins, H.H., de Roos, A.M., 2002. Self-organization of vegetation in arid ecosystems. Amer. Nat. 160 (4), 524–530.
Rietkerk, M., van de Koppel, J., 2008. Regular pattern formation in real ecosystems. Trends Ecol. Evol. 23 (3), 169–175.
Scheffer, M., Bascompte, J., Brock, W.A., Brovkin, V., Carpenter, S.R., Dakos, V., Held, H., van Nes, E.H., Rietkerk, M., Sugihara, G., 2009. Early-warning signals for critical transitions. Nature 461 (7260), 53–59.
Sherratt, J.A., 2013. History-dependent patterns of whole ecosystems. Ecol. Complex. 14, 8–20.
Sherratt, J.A., Mackenzie, J.J., 2016. How does tidal flow affect pattern formation in mussel beds? J. Theoret. Biol. 406, 83–92.
Siero, E., Doelman, A., Eppinga, M., Rademacher, J.D., Rietkerk, M., Siteur, K., 2015. Striped pattern selection by advective reaction–diffusion systems: Resilience of banded vegetation on slopes. Chaos 25 (3), 036411.
Siteur, K., Eppinga, M.B., Karssenberg, D., Baudena, M., Bierkens, M.F., Rietkerk, M., 2014a. How will increases in rainfall intensity affect semiarid ecosystems? Water Resour. Res. 50 (7), 5980–6001.
Siteur, K., Liu, Q.-X., Rottschäfer, V., van der Heide, T., Rietkerk, M., Doelman, A., Boström, C., van de Koppel, J., 2023. Phase-separation physics underlies new theory for the resilience of patchy ecosystems. Proc. Natl. Acad. Sci. 120 (2), e2202683120.
Siteur, K., Siero, E., Eppinga, M.B., Rademacher, J.D., Doelman, A., Rietkerk, M., 2014b. Beyond Turing: The response of patterned ecosystems to environmental change. Ecol. Complex. 20, 81–96.
Tarnita, C.E., Bonachela, J.A., Sheffer, E., Guyton, J.A., Coverdale, T.C., Long, R.A., Pringle, R.M., 2017. A theoretical foundation for multi-scale regular vegetation patterns. Nature 541 (7637), 398–401.
Thiery, J., d'Herbès, J.-M., Valentin, C., 1995. A model simulating the genesis of banded vegetation patterns in Niger. J. Ecol. 497–507.
Thompson, S., Katul, G., McMahon, S.M., 2008. Role of biomass spread in vegetation pattern formation within arid ecosystems. Water Resour. Res. 44 (10).
van de Koppel, J., Crain, C.M., 2006. Scale-dependent inhibition drives regular tussock spacing in a freshwater marsh. Amer. Nat. 168 (5), E136–E147.

van de Koppel, J., Rietkerk, M., Dankers, N., Herman, P.M., 2005. Scale-dependent feedback and regular spatial patterns in young mussel beds. Amer. Nat. 165 (3), E66–E77.

van de Vijsel, R.C., van Belzen, J., Bouma, T.J., van der Wal, D., Cusseddu, V., Purkis, S.J., Rietkerk, M., van de Koppel, J., 2020. Estuarine biofilm patterns: Modern analogues for precambrian self-organization. Earth Surf. Process. Landf. 45 (5), 1141–1154.

van der Heide, T., Bouma, T.J., van Nes, E.H., van de Koppel, J., Scheffer, M., Roelofs, J.G., Van Katwijk, M.M., Smolders, A.J., 2010. Spatial self-organized patterning in seagrasses along a depth gradient of an intertidal ecosystem. Ecology 91 (2), 362–369.

van der Ploeg, M., Appels, W.M., Cirkel, D., Oosterwoud, M., Witte, J.-P., van der Zee, S., 2012. Microtopography as a driving mechanism for ecohydrological processes in shallow groundwater systems. Vadose Zone J. 11 (3).

van der Stelt, S., Doelman, A., Hek, G., Rademacher, J.D., 2013. Rise and fall of periodic patterns for a generalized Klausmeier–Gray–Scott model. J. Nonlinear Sci. 23 (1), 39–95.

van Kampen, N.G., 1976. Stochastic differential equations. Phys. Rep. 24 (3), 171–228.

von Hardenberg, J., Kletter, A.Y., Yizhaq, H., Nathan, J., Meron, E., 2010. Periodic versus scale-free patterns in dryland vegetation. Proc. R. Soc. B: Biol. Sc. 277 (1688), 1771–1776.

Wang, R.-H., Liu, Q.-X., Sun, G.-Q., Jin, Z., van de Koppel, J., 2009. Nonlinear dynamic and pattern bifurcations in a model for spatial patterns in young mussel beds. J. R. Soc. Interface 6 (37), 705–718.

Wasserstein, R.L., Lazar, N.A., 2016. The ASA statement on p-values: context, process, and purpose.

Wasserstein, R.L., Schirm, A.L., Lazar, N.A., 2019. Moving to a world beyond $p < 0.05$.

Weerman, E., Van Belzen, J., Rietkerk, M., Temmerman, S., Kéfi, S., Herman, P., de van de Koppel, J., 2012. Changes in diatom patch-size distribution and degradation in a spatially self-organized intertidal mudflat ecosystem. Ecology 93 (3), 608–618.

Weerman, E.J., van de Koppel, J., Eppinga, M.B., Montserrat, F., Liu, Q.-X., Herman, P.M., 2010. Spatial self-organization on intertidal mudflats through biophysical stress divergence. Amer. Nat. 176 (1), E15–E32.

Yaglom, A., 1962. An Introduction to the Theory of Stationary Random Functions. Prentice-Hall.

Yizhaq, H., Bel, G., 2016. Effects of quenched disorder on critical transitions in pattern-forming systems. New J. Phys. 18 (2), 023004.

Yizhaq, H., Sela, S., Svoray, T., Assouline, S., Bel, G., 2014. Effects of heterogeneous soil–water diffusivity on vegetation pattern formation. Water Resour. Res. 50 (7), 5743–5758.

Yizhaq, H., Stavi, I., Shachak, M., Bel, G., 2017. Geodiversity increases ecosystem durability to prolonged droughts. Ecol. Complex. 31, 96–103.

Zelnik, Y.R., Gandhi, P., Knobloch, E., Meron, E., 2018. Implications of tristability in pattern-forming ecosystems. Chaos 28 (3), 033609.

Zelnik, Y.R., Meron, E., 2018. Regime shifts by front dynamics. Ecol. Indic. 94, 544–552.

Zelnik, Y.R., Meron, E., Bel, G., 2016. Localized states qualitatively change the response of ecosystems to varying conditions and local disturbances. Ecol. Complex. 25, 26–34.

Zelnik, Y.R., Uecker, H., Feudel, U., Meron, E., 2017. Desertification by front propagation? J. Theoret. Biol. 418, 27–35.